Purification and Functional Reconstitution of Monomeric μ-Opioid Receptors

ALLOSTERIC MODULATION OF AGONIST BINDING BY G_{i2} *[S]

Adam J. Kuszak[‡], Sethuramasundaram Pitchiaya[§], Jessica P. Anand[¶], Henry I. Mosberg[¶], Nils G. Walter[§], and Roger K. Sunahara[‡1]

From the Departments of [‡]Pharmacology, [§]Chemistry, and [¶]Medicinal Chemistry, University of Michigan, Ann Arbor, Michigan 48109

Despite extensive characterization of the μ-opioid receptor (MOR), the biochemical properties of the isolated receptor remain unclear. In light of recent reports, we proposed that the monomeric form of MOR can activate G proteins and be subject to allosteric regulation. A μ-opioid receptor fused to yellow fluorescent protein (YMOR) was constructed and expressed in insect cells. YMOR binds ligands with high affinity, displays agonist-stimulated [^{35}S]guanosine 5′-(γ-thio)triphosphate binding to $G\alpha_i$, and is allosterically regulated by coupled G_i protein heterotrimer both in insect cell membranes and as purified protein reconstituted into a phospholipid bilayer in the form of high density lipoprotein particles. Single-particle imaging of fluorescently labeled receptor indicates that the reconstituted YMOR is monomeric. Moreover, single-molecule imaging of a Cy3-labeled agonist, [Lys^7, Cys^8]dermorphin, illustrates a novel method for studying G protein-coupled receptor-ligand binding and suggests that one molecule of agonist binds per monomeric YMOR. Together these data support the notion that oligomerization of the μ-opioid receptor is not required for agonist and antagonist binding and that the monomeric receptor is the minimal functional unit in regard to G protein activation and strong allosteric regulation of agonist binding by G proteins.

Opioid receptors are members of the G protein-coupled receptor (GPCR)[2] superfamily and are clinical mainstays for inducing analgesia. Three isoforms of opioid receptors, μ, δ, and κ, have been cloned and are known to couple to $G_{i/o}$ proteins to regulate adenylyl cyclase and K^+/Ca^+ ion channels

(1–3). An ever growing amount of data suggests that many GPCRs oligomerize (4, 5), and several studies have suggested that μ-opioid receptors (MORs) and δ-opioid receptors heterodimerize to form unique ligand binding and G protein-activating units (6–10). Although intriguing, these studies utilize cellular overexpression systems where it is difficult to know the exact nature of protein complexes formed between the receptors.

To study the function of isolated GPCRs, our laboratory and others have utilized a novel phospholipid bilayer reconstitution method (11–16). In this approach purified GPCRs are reconstituted into the phospholipid bilayer of a high density lipoprotein (HDL) particle. The reconstituted HDL (rHDL) particles are monodispersed, uniform in size, and preferentially incorporate a GPCR monomer (14, 15). Previous work in our lab has shown that rhodopsin, a class A GPCR previously proposed to function as a dimer (17–19), is fully capable of activating its G protein when reconstituted as a monomer in the rHDL lipid bilayer (15). Moreover, we have demonstrated that agonist binding to a monomeric β_2-adrenergic receptor, another class A GPCR, can be allosterically regulated by G proteins (14). This led us to determine whether a monomer of MOR, a class A GPCR that endogenously binds peptide ligands, is the minimal functional unit required to activate coupled G proteins. We additionally investigated whether agonist binding to monomeric MOR is allosterically regulated by inhibitory G protein heterotrimer.

To study the function of monomeric MOR we have purified a modified version of the receptor to near homogeneity. A yellow fluorescent protein was fused to the N terminus of MOR, and this construct (YMOR) was expressed in insect cells for purification. After reconstitution of purified YMOR into rHDL particles, single-molecule imaging of Cy3-labeled and Cy5-labeled YMOR determined that the rHDL particles contained one receptor. This monomeric YMOR sample binds ligands with affinities nearly equivalent to those observed in plasma membrane preparations. Monomeric YMOR efficiently stimulates GTPγS binding to G_{i2} heterotrimeric G protein. G_{i2} allosteric regulation of agonist binding to rHDL·YMOR was also observed. Single-particle imaging of binding of [Lys^7, Cys^8]dermorphin-Cy3, a fluorophore-labeled agonist, to

rHDL·YMOR supports the notion that the rHDL particles contain a single YMOR. Taken together, these results suggest that a monomeric MOR is the minimal functional unit for ligand binding and G protein activation and illustrate a novel method for imaging ligand binding to opioid receptors.

EXPERIMENTAL PROCEDURES

Materials—G protein baculoviruses encoding rat $G\alpha_{i2}$, His_6-$G\beta_1$, and $G\gamma_2$ were provided by Dr. Alfred G. Gilman (University of Texas Southwestern, Dallas, TX). DNA encoding human μ-opioid receptor (NM 000914.2) was provided by Dr. John R. Traynor (University of Michigan, Ann Arbor, MI). Expired serum was generously provided by Dr. Bert La Du (University of Michigan, Ann Arbor, MI). *Spodoptera frugiperda* (Sf9) and *Trichoplusia ni* (HighFive[TM]) cells, pFastBac[TM] baculovirus expression vectors and Sf900[TM] serum-free medium were from Invitrogen. InsectExpress[TM] medium was purchased from Lonza (Allendale, NJ). *N*-Dodecyl-β-D-maltoside was from Dojindo (Rockville, MD). All of the lipids were from Avanti Polar Lipids (Alabaster, AL). [^{3}H]diprenorphine (DPN, 54.9 Ci/mmol) and [^{35}S]GTPγS (1250 Ci/mmol) were obtained from PerkinElmer Life Sciences. EZ-Link[TM] NHS-Biotin reagent was from Pierce. Ovomucoid trypsin inhibitor was purchased from United States Biological (Swampscott, MA). GF/B and BA85 filters, Cy3 and Cy5 NHS-ester mono-reactive dyes, Cy3-maleimide dye, and Source 15Q and Superdex 200 chromatography resins were from GE Healthcare. Talon[TM] resin was from Clontech. Bio-Beads[TM] SM-2 absorbant resin was from Bio-Rad. Chromatography columns were run using a BioLogic Duo-Flow protein purification system from Bio-Rad. Amicon Ultra centrifugation filters were from Millipore (Billerica, MA). Amino acids for ligand synthesis were obtained from Advanced ChemTech (Louisville, KY) or Sigma-Aldrich. All other chemicals and ligands were from either Sigma-Aldrich or Fisher Scientific.

YFP-μ-Opioid Receptor Fusion Protein Expression and Purification—Baculoviruses were created using transfer vectors (pFastBac[TM]) that encoded a fusion protein of an N-terminal cleavable hemagglutinin signal sequence (MKTIIALSYIFCLVF), a FLAG epitope (DYKDDDD), a decahistidine tag, the monomeric and enhanced yellow fluorescent protein (Clontech), and the human MOR. High titer viruses (10^7–10^8 plaque-forming units/ml) were used to infect Sf9 or HighFive[TM] suspension cultures at a multiplicity of infection of 0.25 to 1. FLAG-His_{10}-mEYFP-MOR (YMOR) was expressed for 48–52 h in the presence of 1 μM naltrexone (NTX). The cells were resuspended in Buffer A (50 mM Tris·HCl, pH 8.0, 50 mM NaCl, 100 nM NTX, and protease inhibitors (3.2 μg/ml leupeptin, 3.2 μg/ml ovomucoid trypsin inhibitor, 17.5 μg/ml phenylmethanesulfonyl fluoride, 16 μg/ml tosyl-L-lysine-chloromethyl ketone (TLCK), 16 μg/ml tosyl-L-phenylalanine chloromethyl ketone (TPCK)) and lysed by nitrogen cavitation. Supernatants from a 500 × g spin were then subjected to 125,000 × g spin for 35 min, and pellets containing membrane fractions were resuspended in Buffer A and either stored at −80 °C for later binding assays or further processed to purify receptor.

All of the purification steps were performed sequentially and at 4 °C or on ice. Membrane preparations were diluted to 5 mg/ml in Buffer A plus 1% DDM (w/v) and 0.01% cholesteryl hemisuccinate (CHS) (w/v) and gently stirred for 1 h to solubilize YMOR out of the membrane. Detergent extracted YMOR was enriched via Talon[TM] metal affinity chromatography resin (Clontech) in Buffer A plus 0.1% DDM and 0.01% CHS and eluted with Buffer A plus 0.1% DDM, 0.01% CHS, and 150 mM imidazole. Fractions containing YMOR (based on Coomassie staining after SDS-PAGE separation) were pooled, diluted 5-fold in Buffer B (20 mM Hepes, pH 8.0, 5 mM $MgCl_2$, 0.1% DDM, 0.01% CHS, 100 nM NTX, and phenylmethanesulfonyl fluoride-TLCK-TPCK protease inhibitors), and eluted from a 1-ml Source 15Q strong anion exchange column with a 50–300 mM NaCl linear gradient. Peak fractions were identified by radioligand binding assays using [^{3}H]DPN (2–4 nM). Peak fractions were then pooled and concentrated on Amicon Ultra centrifugation filters (10-kDa molecular mass cut-off). As a final purification step this YMOR sample was resolved based on size using a Superdex 200 gel filtration column (GE Healthcare) in Buffer C (20 mM Hepes, pH 8.0, 100 mM NaCl, 0.1% DDM, 0.01% CHS, 100 nM NTX, and protease inhibitors). Coomassie staining after SDS-PAGE was used to identify fractions containing YMOR, which were pooled and concentrated to ~1–2 μM. Glycerol was added to a final concentration of 10% (v/v), and the samples were flash-frozen in liquid nitrogen and then stored at −80 °C until further use.

ApolipoproteinA-1 Purification—Wild type human apoA-1 was purified from expired serum as previously described (14). A recombinant apoA-1 with an N-terminal 43-amino acid deletion and a histidine tag ($\Delta(1–43)$-His_6-ApoA-1) was expressed using a pET15b vector to transform competent *Escherichia coli* cells (BL21). The cells were resuspended and lysed by gentle vortexing in 10 mM Tris·HCl, pH 8.0, 100 mM NaH_2PO_4, 6 M guanidine hydrochloride, 1% Triton X-100. Lysate was fractionated by centrifugation at 10,000 × g, and the supernatant was loaded onto a nickel-nitrilotriacetic acid column by gravity flow. The column was washed with 10 mM Tris·HCl, pH 8.0, 100 mM NaH_2PO_4, 6 M guanidine hydrochloride, 1% Triton X-100 and then with 50 mM NaH_2PO_4, pH 8.0, 300 mM NaCl, 1% Triton X-100. Bound $\Delta(1–43)$-His_6-apoA-1 was eluted with 50 mM NaH_2PO_4, pH 8.0, 300 mM NaCl, 250 mM imidazole, 1% Triton X-100. Peak fractions were further purified on a Superdex 75 gel filtration chromatography column in 20 mM Hepes, pH 8.0, 100 mM NaCl, 1 mM EDTA, 20 mM sodium cholate. Pooled apoA-1 was then dialyzed against 20 mM Hepes, pH 8.0, 100 mM NaCl, 1 mM EDTA, 5 mM sodium cholate. Purified apoA-1 was concentrated to ~10 mg/ml and stored at −80 °C until use.

In Vitro HDL Reconstitution—HDL particles were reconstituted according to previously reported protocols (14). Briefly, 21 mM sodium cholate, 7 mM lipids (1-palmitoyl-2-oleoyl-*sn*-glycero-3-phosphocholine (POPC) and 1-palmitoyl-2-oleoyl-*sn*-glycero-3-[phospho-*rac*-(1-glycerol)] (POPG) at a molar ratio of 3:2), purified YMOR (DDM-solubilized), and 100 μM purified apoA-1 were solubilized in 20 mM Hepes, pH 8.0, 100 mM NaCl, 1 mM EDTA, 50 mM sodium cholate. The final concentration of YMOR varied from 0.2 to 0.4 μM, but YMOR

Functional G Protein Coupling by μ-Opioid Receptor Monomer

always comprised 20% of the total reconstitution volume. In some reconstitutions the lipid component was modified such that porcine polar brain lipid extract (Avanti Polar Lipids) was used in addition to POPC and POPG for a final concentration of 7 mM lipids at a molar ratio of 1.07:1.5:1 brain lipid:POPC:POPG. Following incubation on ice (1.5–2 h), the samples were added to Bio-Beads™ (Bio-Rad, 0.05 mg/ml of reconstitution volume) to remove detergent and to form HDL particles. Particles containing YMOR were purified via M1 anti-FLAG immunoaffinity chromatography resin (Sigma) and eluted with 1 mM EDTA plus 200 μg/ml FLAG peptide. To assess the efficiency of HDL reconstitution, the total protein concentration of rHDL·YMOR was compared with the concentration of active reconstituted YMOR. FLAG affinity column-purified rHDL·YMOR was resolved from BSA and FLAG peptide on a Superdex 200 gel filtration column, and the peak fraction was analyzed for protein content with Amido Black staining (20), whereas [³H]DPN saturation assays were used to measure active YMOR content. YMOR reconstituted into HDL was stored on ice until further use.

G Protein Addition to rHDL·YMOR Particles—G_{i2} heterotrimer ($G\alpha_{i2}$-His$_6$Gβ_1-Gγ_2) was expressed in Sf9 cells and purified as previously described (21). The concentration of active G protein was determined by filter binding of 20 μM [³⁵S]GTPγS (isotopically diluted) in 30 mM NaHepes, pH 8.0, 100 mM NaCl, 50 mM MgCl$_2$, 1 mM EDTA, 0.05% C$_{12}$E$_{10}$, and 1 mM dithiothreitol after 1 h of incubation at room temperature. Purified G protein heterotrimer was added to preformed, FLAG-purified rHDL·YMOR particles at a molar ratio of 1:10 receptor to G protein. G_{i2} was purified in 0.7% CHAPS, and the final volume of G protein added to rHDL·YMOR was such that the final CHAPS concentration was well below its critical micelle concentration. Reconstituted receptor and G protein samples were then incubated in Bio-Beads™ for 30–45 min at 4 °C to remove residual detergent.

[³H]DPN Saturation and Agonist Competition Binding Assays—Binding reactions were performed in 100-μl volumes. Membrane fractions prepared from Sf9 or HighFive™ cells expressing YMOR (0.5–5 μg total protein, prepared as above) were incubated with [³H]DPN (0.25 to 4 nM; 54.9 Ci/mmol) for 1 h at room temperature in 25 mM Tris·HCl, pH 7.7, 136 mM NaCl, 2.7 mM KCl (Tris-buffered saline) buffer. Nonspecific binding was determined in the presence of 20 μM NTX. Bound [³H]DPN was separated from free by rapid filtration through GF/B filters and three 200-μl washes of ice-cold Tris-buffered saline. [³H]DPN saturation binding reactions on YMOR incorporated into rHDL particles were prepared in Tris-buffered saline, pH 7.7, plus 0.1% BSA, and Sephadex G-50 Fine (GE Healthcare) gravity flow columns were used to separate bound from free [³H]DPN. Agonist competition assays in insect membranes and rHDL particles were performed in 25 mM Tris·HCl, pH 7.7, 6–7 mM NaCl. Competition assays in rHDL particles also included 0.1% BSA. [³H]DPN binding assays on detergent-solubilized YMOR were performed in 50 mM Tris·HCl, pH 7.7, 136 mM NaCl, 0.1% DDM, 0.01% CHS and separated on Sephadex G-50 gravity flow columns. For agonist competition assays, receptor samples were incubated with 0.5–1 nM [³H]DPN and increasing concentrations of agonist (1 pM to 1

mM) in the absence or presence of 10 μM GTPγS. The samples were measured for radioactivity on a liquid scintillation counter, and the data were fit with one-site saturation, one-site competition, or two-site competition binding models using Prism 5.0 (GraphPad, San Diego, CA).

[³⁵S]GTPγS Binding Assay—100-μl volume reactions were prepared containing 1 μg of total membrane protein from YMOR expressing HighFive™ cells or ~50–60 fmol of YMOR incorporated into rHDL particles in 30 mM Tris·HCl, pH 7.4, 100 mM NaCl, 5 mM MgCl$_2$, 0.1 mM dithiothreitol, 10 or 1 μM GDP (membranes or HDL particles), and 0.1% BSA. Membrane assays and rHDL assays were incubated with 10 nM isotopically diluted [³⁵S]GTPγS (12.5 Ci/mmol). YMOR samples were incubated with increasing concentrations of agonists (1 pM to 1 mM) for 1 h at room temperature, then rapidly filtered through GF/B (membrane samples) or BA85 filters (HDL samples), and washed three times with 2 ml of ice-cold 30 mM Tris·HCl, pH 7.4, 100 mM NaCl, 5 mM MgCl$_2$. The samples were measured for radioactivity on a liquid scintillation counter, and the data were fit with a log dose-response model using Prism 5.0.

Single-molecule Imaging of Reconstituted Cy3- and Cy5-YMOR—Purified YMOR (~200 pmol) was incubated with NHS-ester Cy3 or Cy5 mono-reactive dye (GE Healthcare) in 20 mM Hepes, pH 8.0, 100 mM NaCl, 5 mM MgCl$_2$, 6 mM EDTA, 0.1% DDM, 0.01% CHS, 100 nM NTX for 30 min at 25 °C and then 1 h at 4 °C. Conjugation reactions were quenched by the addition of Tris·HCl, pH 7.7 buffer (10 mM final). Cy-labeled YMOR was then separated from free dye using a 12-cm Sephadex G-50 column. The final dye to protein molar ratio was 3.8:1 for Cy3-YMOR and 3.7:1 for Cy5-YMOR, determined by absorbance at 280 nm for total protein, 550 nm for Cy3 dye, and 650 nm for Cy5 dye as measured on a NanoDrop ND-1000 spectrophotometer. A separate aliquot of YMOR was co-labeled with both Cy3 and Cy5 for final molar ratios of 2:1 Cy3:YMOR and 1.8:1 Cy5:YMOR. HDL reconstitutions of Cy3-YMOR alone, Cy5-YMOR alone, a mixture of Cy3- and Cy5-YMOR, and Cy3-Cy5-YMOR were then performed. Reconstitutions were performed as previously described, using apoA-1 that had been biotinylated at a 3:1 molar ratio using EZ-Link NHS-Biotin according to the manufacturer's protocol (Pierce). Reconstituted samples were diluted 5000-fold in 25 mM Tris·HCl, pH 7.7, and injected into a microfluidic channel on a quartz slide that was previously coated with biotinylated polyethylene glycol and treated with 0.2 mg/ml streptavidin to generate a surface density of ~0.05 molecules/μm². An oxygen scavenging system of 10 mM Trolox (Sigma-Aldrich), 100 mM protocatechuic acid, and 1 μM protocatechuate-3,4-dioxygenase was included in the sample dilution (22). Following a 10-min incubation to allow binding of the biotin-HDL·Cy-YMOR complex to the streptavidin-coated slide, the channel was washed with ice-cold 25 mM Tris·HCl, pH 7.7, containing the oxygen scavenging system. An Olympus IX71 inverted microscope configured for prism-based total internal reflection fluorescence (TIRF) and coupled to an intensified CCD camera was used to image Cy3 and Cy5 fluorophores (CrystaLaser, 532 nm; Coherent CUBE laser, 638 nm; Chroma band pass filters HQ580/60 and HQ710/130 nm). Fluorophore intensity time
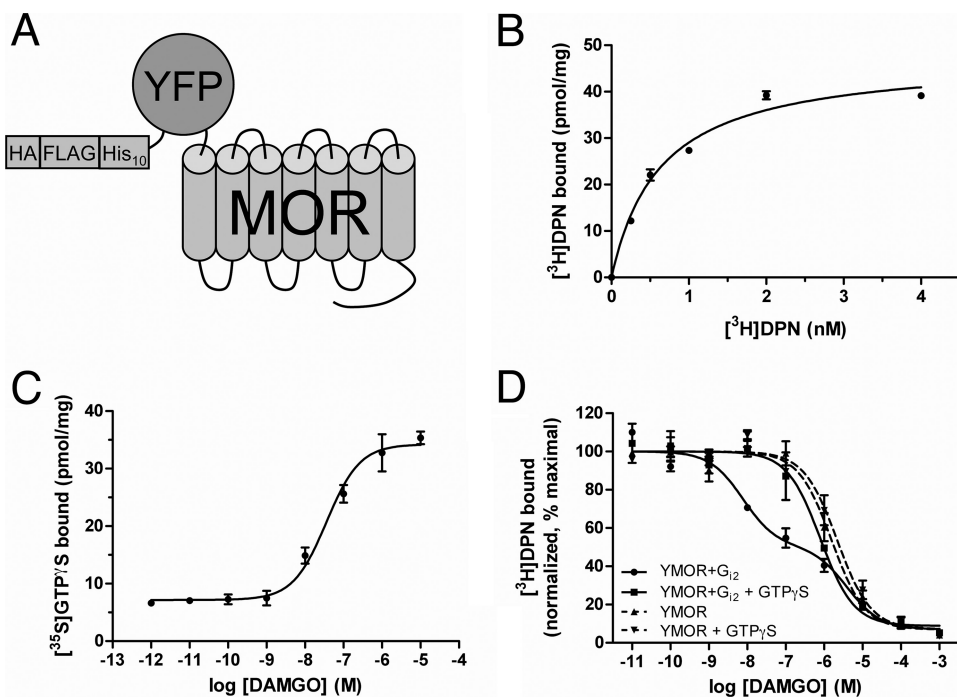
FIGURE 1. **Functional expression of a modified MOR in insect cells.** *A*, schematic representation of the modified μ-opioid receptor expressed in insect cells. N-terminal modifications included a hemagglutinin signal sequence (*HA*), FLAG epitope, His_{10}, and a YFP. This construct, termed YMOR, was expressed in Sf9 and HighFive[TM] insect cells using a recombinant Baculovirus system. *B*, YMOR expressed in insect cells exhibits high affinity ligand binding. Plasma membrane preparations (5 μg) of HighFive[TM] cells expressing YMOR were used in [^{3}H]diprenorphine saturation binding assays. YMOR bound [^{3}H]DPN with a B_{max} of ~40 pmol/mg and a K_d of 0.6 ± 0.1 nM. *C*, YMOR couples to G protein in insect cell membranes. Membrane preparations (2 μg) of HighFive[TM] cells co-expressing YMOR and G_{i2} heterotrimer were incubated with increasing concentrations of the μ-opioid agonist DAMGO in the presence of 10 nM [^{35}S]GTPγS (isotopically diluted). DAMGO stimulated [^{35}S]GTPγS exchange on $G\alpha_{i2}$ with an EC_{50} of 36 ± 0.1 nM. *D*, agonist binding to YMOR expressed in insect cells is allosterically regulated by G proteins. YMOR/G_{i2} membrane preparations (2–3 μg) were incubated with 0.8 nM [^{3}H]DPN and increasing concentrations of DAMGO in the absence or presence of 10 μM GTPγS. A high affinity binding site for DAMGO (●, $K_{i hi}$ = ~2.9 nM) was disrupted in the absence of G protein coupling (with GTPγS, ■, K_i = ~300 nM). DAMGO also displayed low affinity binding to membranes not expressing G_{i2} (YMOR, ▲, K_i = ~580 nM; and YMOR + GTPγS, ▼, K_i = ~800 nM). Binding data were normalized to the curve fit maximum. For all panels the data are representative of at least two experiments performed in duplicate, and the *error bars* represent the standard error of the mean.

traces were collected for 30–100 s at 10 frames/s. Time traces were analyzed for photobleaching with in-house software (MatLab 7.0).

Synthesis of [Lys[7], Cys[8]]Dermorphin and Labeling with Cy3 Dye—[Lys[7], Cys[8]]dermorphin (Tyr-D-Ala-Phe-Gly-Tyr-Pro-Lys-Cys-NH$_2$) was synthesized on Rink resin (solid support) using an Applied Biosystems 431A peptide synthesizer and standard Fmoc (*N*-(9-fluorenyl)methoxycarbonyl) chemistry. The samples were characterized on a Waters reverse phase HPLC using a Vydac C18 (Protein and Peptide) 10-micron column. The samples were run on a linear gradient of 0–45% acetonitrile in an aqueous phase containing 0.1% trifluoroacetic acid at 35 °C and monitored at 254 and 230 nm (supplemental Fig. S3). Peptides were similarly purified on a Waters semipreparative reverse phase HPLC using a Vydac C18 10-micron column at room temperature. The purified peptide was labeled with Cy3-maleimide (GE Healthcare) according to the manufacturer's instructions using a ratio of 1.5:1 peptide to fluorophore and repurified by HPLC as before. The labeled peptide was further purified via semi-preparative HPLC using a 5-micron Vydac C18 column as described above. The potency and efficacy of [Lys[7], Cys[8]]dermorphin-Cy3 at MOR were con-

firmed in radiolabeled [^{3}H]DPN competition and [^{35}S]GTPγS binding assays.

Prism-based Single-molecule TIRF and Step Photobleaching Analysis of [Lys[7], Cys[8]]Dermorphin-Cy3 Binding to rHDL·YMOR + G_{i2}—Purified recombinant apoA-1 was biotinylated at a 3:1 molar ratio of biotin:apoA-1. Purified YMOR was then reconstituted with biotin-apoA-1, POPC, POPG, and brain lipid extract as above. Purified G_{i2} heterotrimer was added to reconstituted receptor as above, and coupling was confirmed by observing high affinity competition of [^{3}H]DPN binding by the agonist DAMGO. Five nanomolar biotin-rHDL·YMOR+G_{i2} was then incubated with 5 μM [Lys[7], Cys[8]]-dermorphin-Cy3 for 45 min at 25 °C in 25 mM Tris·HCl, pH 7.7. The samples were diluted 100-fold in 25 mM Tris·HCl, pH 7.7, and imaged as described above with a surface density of ~0.25 molecules/μm[2]. Fluorophore intensity time traces were collected for 30–100 s at 10 frames/s and analyzed for photobleaching with in-house software (MatLab 7.0).

RESULTS

Expression of a Functional μ-Opioid Receptor Fusion Protein in Insect Cells—Human YMOR (Fig. 1*A*) expressed in Sf9 and High-Five[TM] insect cells bound the nonspecific opioid antagonist [^{3}H]diprenorphine ([^{3}H]DPN) with high affinity in a saturable manner (K_d = 0.6 ± 0.1 nM; Fig. 1*B*). Maximal receptor levels of 12–40 pmol/mg were routinely observed.

The μ-selective agonist DAMGO ([D-Ala[2], N-MePhe[4], Gly[5]-ol]enkephalin) stimulated [^{35}S]GTPγS binding to membranes co-expressing YMOR and $G\alpha_{i2}$-His$_6$Gβ_1-Gγ_2 G protein heterotrimer (G_{i2}) in a concentration-dependent manner (Fig. 1*C*). DAMGO elicited strong activation of G_{i2}, stimulating [^{35}S]GTPγS binding nearly 4-fold over basal levels with an EC_{50} of 36 ± 0.1 nM. The potency and efficacy of DAMGO at insect cell expressed YMOR is well in line with its observed pharmacological characteristics in mammalian cell expression systems (23–25).

Allosteric regulation of agonist binding to opioid receptors by G proteins has been well established in plasma membrane preparations of brain homogenates and overexpression systems (26–30) and was also observed for YMOR expressed in insect cells. In the absence of G_{i2}, DAMGO competed [^{3}H]DPN (0.5 nM) binding in a concentration-dependent manner with a K_i of ~580 nM (Fig. 1*D*). In membranes expressing both YMOR and

Functional G Protein Coupling by μ-Opioid Receptor Monomer

A

B

C
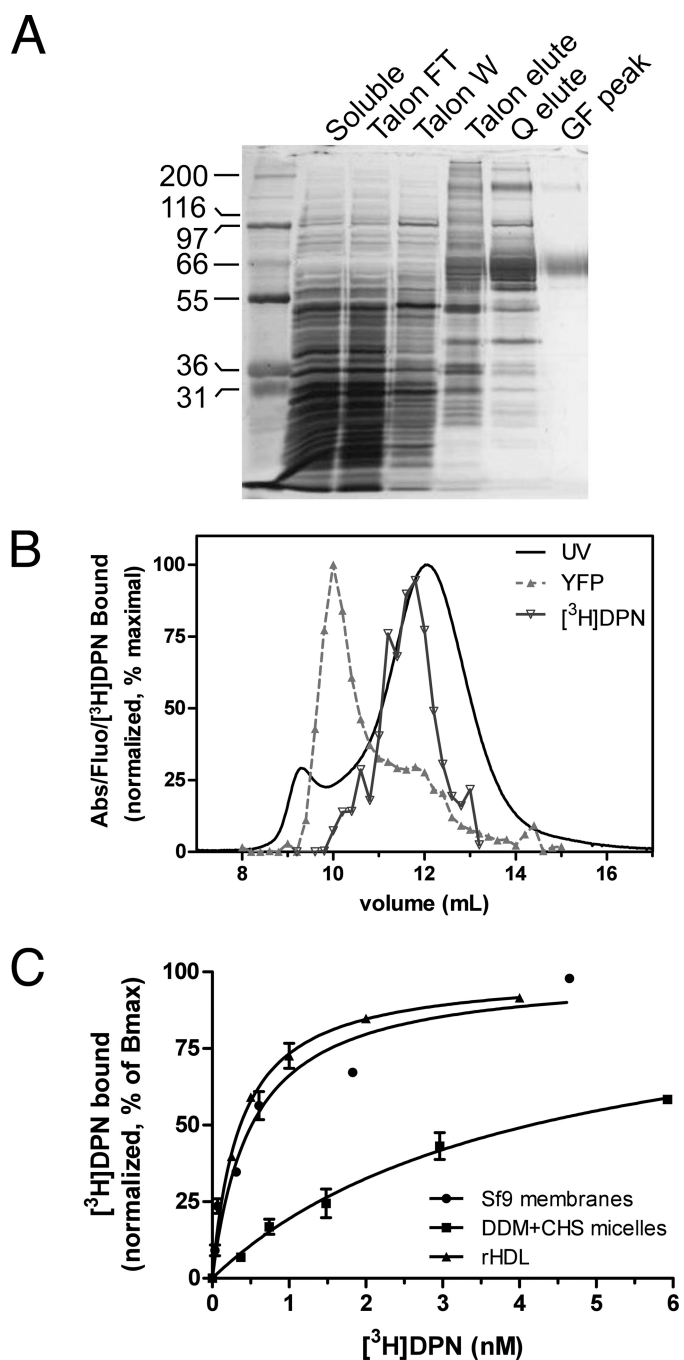
FIGURE 2. **Purification of YMOR from HighFive[TM] insect cells and reconstitution into HDL particles.** *A*, YMOR was extracted from membranes in the presence of 100 nM naltrexone with 1% *n*-dodecyl-β-D-maltoside and 0.01% cholesteryl hemisuccinate and enriched on a Talon[TM] metal affinity column. The Talon[TM] pool containing YMOR (predicted 73-kDa molecular mass) was applied to a Source 15Q anion exchange column followed by a size exclusion gel filtration column (Superdex 200). Samples of the purification steps were resolved by SDS-PAGE and silver-stained. YMOR was enriched to ~95% purity (GF peak). *B*, purified YMOR was reconstituted into HDL particles (see "Experimental Procedures") and resolved by size exclusion chromatography (Superdex 200). Fractions were analyzed for total protein content (UV absorbance), active YMOR ([³H]DPN binding), and YFP fluorescence. UV absorbance showed a major peak corresponding to rHDL particles (stokes diameter of ~10.5 nm). The elution volume of active YMOR corresponded with the rising slope of the rHDL peak. YFP fluorescence eluted as two peaks, corresponding to the active YMOR and a larger YMOR aggregate that was not incorporated into rHDL particles. This aggregated YMOR was not active based on [³H]DPN binding. The data were normalized such that the maximal value for each parameter was set to 100%. [³H]DPN binding measurements were performed

Gi_2, DAMGO exhibited a biphasic mode of inhibition of [³H]DPN binding with a $K_{i\,hi}$ of ~2.9 nM and a $K_{i\,lo}$ of ~1.5 μM (fraction of $K_{i\,hi}$ ~0.53). The addition of 10 μM GTPγS to the YMOR + Gi_2 membranes eliminated the high affinity DAMGO-binding site (K_i = ~300 nM), illustrating that YMOR is allosterically regulated by G proteins. Therefore, YMOR expressed in HighFive[TM] cells proved fully functional in regards to G protein coupling.

YMOR Purification—The capacity of a variety of detergents (zwitterionic, polar, and nonionic detergents such as Triton X-100, digitonin, Nonidet P-40, CHAPS, $C_{12}E_{10}$, and *n*-octyl-β-glucoside) to solubilize YMOR from insect cell membranes was assessed by anti-FLAG Western blot analysis. Extraction of YMOR with DDM proved to be most efficient (data not shown). The addition of CHS (0.01% w/v) improved the stability of the solubilized receptor as measured by [³H]DPN binding, consistent with the stabilizing effects of cholesterol moieties observed for solubilized $β_2$AR (31) (supplemental Fig. S1). The expression levels of YMOR and the efficiency of DDM solubilization, assessed by [³H]DPN binding and anti-FLAG Western blots, were enhanced in the presence of naltrexone. Therefore this antagonist was present (100 nM) during all subsequent purification steps.

DDM-extracted YMOR was purified through a series of chromatographic steps including metal chelate (Talon[TM]), anion exchange (Source 15Q), and size exclusion (Superdex 200) chromatography columns. Peak fractions from each column were determined by Coomassie staining, anti-FLAG antibody Western blotting, and [³H]DPN binding. Fractions displaying the highest [³H]DPN binding capacity and appropriate molecular weight were pooled and subjected to the next chromatographic step. Superdex 200 peak fractions were pooled, concentrated, flash-frozen in liquid N_2, and then stored at −80 °C until later use. A representative silver-stained SDS-PAGE separation of each enrichment step is shown in Fig. 2*A*. Yields of YMOR were typically ~50 μg of >95% pure receptor/liter of insect culture. YMOR, deemed pure based on silver staining, bound [³H]DPN at ~20% of the predicted binding sites calculated from the molecular mass. This loss of activity is likely due to the detrimental freeze/thaw process.

Reconstitution of YMOR into High Density Lipoprotein Particles—The reconstitution of YMOR into high density lipoprotein (rHDL) particles was performed with a 500-fold molar excess of apoA-1 to YMOR (250-fold excess of rHDL) to favor reconstitution of a single YMOR molecule/rHDL particle. Resolution of rHDL particles containing YMOR (rHDL·YMOR) with size exclusion chromatography (SEC) suggested an apparent Stokes diameter of 10.5 nm (Fig. 2*B*). [³H]DPN binding to the SEC fractions confirmed the presence of func-

in duplicate, and the *error bars* are omitted for clarity. *C*, high affinity [³H]DPN binding to YMOR is disrupted in detergent micelles but restored following reconstitution into rHDL particles. [³H]DPN binding to YMOR in insect cell membranes (●, K_d = ~0.5 nM), purified in DDM micelles (■, K_d = ~4.1 nM), and in rHDL particles (▲, K_d = ~0.4 nM). The data are representative of at least three experiments performed in duplicate, and the *error bars* represent the standard error of the mean. The binding data were normalized to the maximal binding level (B_{max}) as calculated by a one-site saturation curve fit (Prism 5.0, GraphPad).

tional YMOR in particles that eluted slightly earlier than the main UV absorbance peak (Stokes diameter of ~10.3 nm), indicating the slightly larger size of rHDL·YMOR compared with rHDL. The YFP fluorescence of the SEC fractions indicated an additional peak that elutes near in the Superdex 200 void volume, suggestive of aggregated YMOR. Because these fractions did not bind [³H]DPN, we surmised that this receptor population was inactive. This aggregated and inactive receptor is consistent with the previous observation that ~80% of the purified YMOR is inactive post freeze/thaw and prior to reconstitution into HDL.

The effectiveness of YMOR reconstitution into HDL is clear when comparing [³H]DPN binding between detergent-solubilized receptor and rHDL·YMOR particles. Prior to reconstitution into HDL, DDM-soluble YMOR bound [³H]DPN with a K_d of ~4.1 nM, whereas reconstituted YMOR bound [³H]DPN with a K_d of ~0.4 nM (Fig. 2C). This significant disruption of high affinity ligand binding for the soluble receptor is not surprising, because detergents are known to decrease the ligand affinity of opioid receptors (32) and disrupt GPCRs in general (33). Replacement of detergents with phospholipids reverses the deleterious effects of the detergent and restores YMOR conformation to one that binds [³H]DPN with native, membrane-bound affinity.

YMOR Is Monomeric When Incorporated into rHDL—To determine the number of YMOR molecules present in each rHDL particle, we assessed the degree of receptor co-localization between Cy3- and Cy5-labeled YMOR using single-particle imaging. Purified YMOR was labeled with Cy3- or Cy5-reactive fluorescent dyes and reconstituted into HDL using biotinylated Δ(1–43)-His₆-apoA-1. This biotin-rHDL·Cy-YMOR complex was then incubated on a streptavidin-coated microfluidic slide and excited with 532- and 638-nm lasers. Fluorescence emission was detected using prism-based SM-TIRF. Reconstituted Cy3-YMOR and Cy5-YMOR were visualized as mono-disperse fluorescent foci (Fig. 3, *A* and *B*). When Cy3-YMOR and Cy5-YMOR were mixed prior to reconstitution (Cy3-YMOR+Cy5-YMOR), a low level of co-localization of the two fluorophores (3.4%) was observed (Fig. 3, *C* and *E*). A false-positive co-localization signal of 2.8 and 2.2% was observed for the Cy3-YMOR and Cy5-YMOR samples, respectively (Fig. 3*E*). As a positive control, co-localization for YMOR labeled with both Cy3 and Cy5 was also measured (Fig. 3*D*). Considering that our method does not allow for the differentiation between YMOR labeled with multiple Cy probes of the same fluorophore *versus* co-localization of multiple YMORs labeled with the same Cy probe, we may underestimate co-localization by as much as a factor of 2. Thus we estimate an upper limit for co-localization, *i.e.* incorporation of two or more YMORs into a single rHDL particle, of ~1.8% ((3.4% × 2) − (2.8% + 2.2%)). These data suggest that HDL reconstitution resulted in a sample containing mostly monomeric YMOR. Therefore the ligand binding and G protein coupling characteristics of the HDL-reconstituted YMOR presented here are indicative of the properties of a monomeric receptor.

To assess the amount of active *versus* inactive YMOR incorporated into rHDL, we compared the total protein concentration of purified rHDL·YMOR particles to the maximal concen-
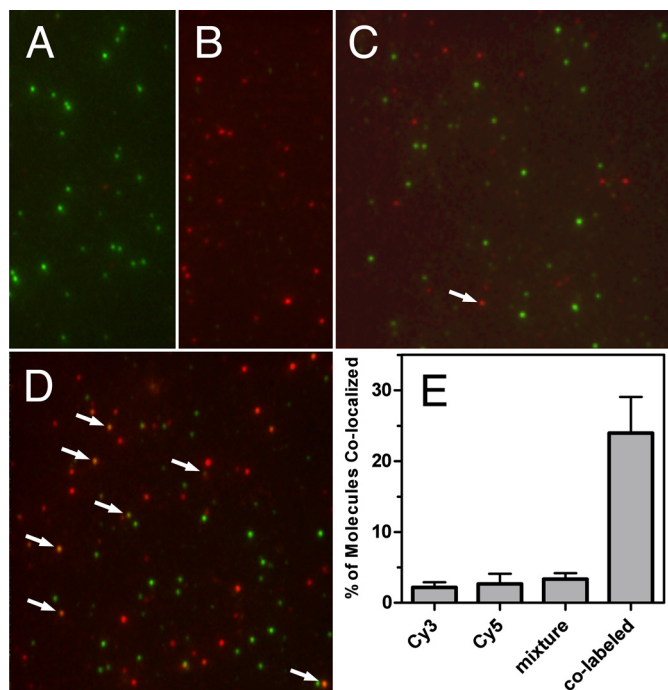
FIGURE 3. **YMOR is monomeric when reconstituted into HDL particles.** Purified YMOR was labeled with Cy3 or Cy5 fluorescent dyes and reconstituted separately or together into biotin-labeled rHDL. The particles were imaged using single-molecule total internal reflection fluorescence microscopy on quartz slides coated with streptavidin. Representative overlay images of reconstituted rHDL·Cy3-YMOR (*A*), rHDL·Cy5-YMOR (*B*), rHDL·(Cy3-YMOR + Cy5-YMOR) (*C*), and rHDL·Cy3-Cy5-YMOR (*D*) are shown. Quantification of Cy3 and Cy5 co-localization (*E*) showed that when both Cy3-YMOR and Cy5-YMOR were mixed together prior to reconstitution (mixture, 4c), only ~3.4% of rHDL particles contained two labeled receptors, compared with a false-positive co-localization signal of 2.8 and 2.2% observed for the rHDL·Cy3-YMOR and rHDL·Cy5-YMOR samples. YMOR co-labeled with both Cy3 and Cy5 was also imaged as a positive control for co-localization. Approximately 24% of rHDL·Cy3-Cy5-YMOR particles (co-labeled, 4d) exhibited co-localization, indicating that not all YMOR received a secondary fluorescent dye under the labeling conditions.

tration of YMOR based on [³H]DPN saturation binding assays. Reconstituted YMOR was purified using FLAG affinity resin and resolved by SEC into a sample containing only apoA-1 and YMOR (based on SDS-PAGE and Coomassie staining). Amido Black staining of these peak fractions indicated a protein concentration of ~5.2 μg/ml. Considering that the protein sample consists of two apoA-1 molecules (molecular mass, ~25,500 Da) and one YMOR (molecular mass, ~73,500 Da), the rHDL·YMOR sample has a total molecular mass of 124,500 Da and therefore a molar concentration of ~42 nM. Saturation binding assays on the rHDL·YMOR SEC peak indicated a molar concentration of ~31 nM for YMOR which bound ligand. Given the inherent limitations of protein detection assays at the low concentration of our samples, these data suggest that at least 75% of the YMOR in rHDL is active based on [³H]DPN binding.

Monomeric YMOR Binds Antagonists with High Affinity—Reconstituted and monomeric YMOR binds antagonists with affinities similar to those observed in the plasma membrane. The antagonists naloxone and naltrexone and the μ-specific peptide CTAP (D-Phe-Cys-Tyr-D-Trp-Arg-Thr-Pen-Thr-NH₂) compete [³H]DPN binding in similar fashion when in HighFive™ cell membrane preparations or in reconstituted

Functional G Protein Coupling by μ-Opioid Receptor Monomer
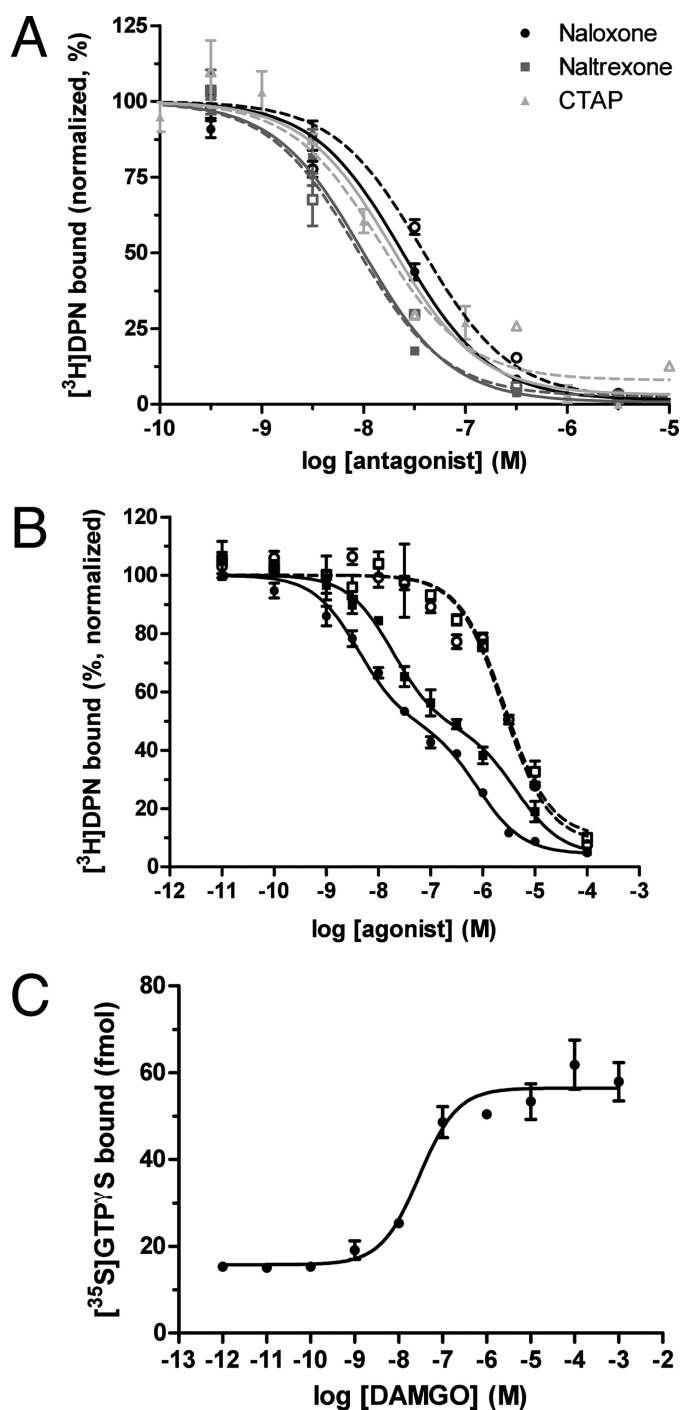
FIGURE 4. **Monomeric YMOR binds ligands with high affinity and functionally couples to G_{i2} heterotrimer.** *A*, opioid antagonists bind YMOR in rHDL with affinities equivalent to those observed in membrane preparations. Competition binding assays were performed using plasma membranes of HighFive[TM] cells expressing YMOR and G_{i2} heterotrimer (*dotted lines*, *open symbols*) or rHDL·YMOR (*solid lines*, *closed symbols*). For CTAP binding assays in rHDL, YMOR was coupled to G_{i2} heterotrimer. Increasing concentrations of naloxone, naltrexone, or CTAP competed the binding of 1 nM [^{3}H]DPN in the rHDL system or 0.5 nM [^{3}H]DPN in membrane preparations. The observed binding constants were: naloxone $K_{i\,mem} = \sim19$ nM, $K_{i\,rHDL} = \sim7.8$ nM; naltrexone $K_{i\,mem} = \sim4.3$ nM, $K_{i\,rHDL} = \sim3.3$ nM; CTAP $K_{i\,rHDL} = \sim7.1$ nM, $K_{i\,rHDL} = \sim7.6$ nM. *B*, binding of morphine to rHDL·YMOR is allosterically regulated by G proteins. Purified G_{i2} heterotrimer was added to rHDL·YMOR at a molar ratio of 10:1, G protein to receptor. DAMGO and morphine bound rHDL·YMOR with high affinity, competing the binding of 0.75 nM [^{3}H]DPN in a biphasic manner (DAMGO (■), $K_{i\,hi} = \sim7.6$ nM, $K_{i\,lo} = \sim1.8$ μM; morphine (●), $K_{i\,hi} = \sim1.7$ nM, $K_{i\,lo} = \sim320$ nM). High affinity agonist binding was lost with the addition of

HDL particles (Fig. 4*A*). Therefore reconstitution into HDL allows YMOR to adopt a conformation that appears identical to receptor in plasma membranes in terms of high affinity antagonist binding.

Monomeric YMOR Functionally Couples Inhibitory G Proteins—We next analyzed the capacity of monomeric YMOR to functionally couple to heterotrimeric G protein. Functional measurements included allosteric regulation of agonist binding (Fig. 4*B*) and agonist-mediated stimulation of [^{35}S]GTPγS binding (Fig. 4*C*). Anti-FLAG affinity column purification of rHDL·YMOR was performed to remove "empty" rHDL particles, and purified G_{i2} heterotrimer was added at a 10:1 G_{i2}: rHDL·YMOR molar ratio. The concentration of purified G protein was determined by [^{35}S]GTPγS binding assays, and receptor concentration was measured with [^{3}H]DPN saturation assays of rHDL·YMOR samples. G_{i2} addition results in high affinity agonist binding (Fig. 4*B*). Morphine competed [^{3}H]DPN binding with a $K_{i\,hi}$ of ~1.7 nM and a $K_{i\,lo}$ of ~320 nM, whereas DAMGO inhibited with a $K_{i\,hi}$ of ~7.6 nM and a $K_{i\,lo}$ of ~1.8 μM. As in membranes the addition of 10 μM GTPγS to the monomeric rHDL·YMOR+G_{i2} uncouples the G protein and results in a single-site, low affinity agonist competition curve. Similarly, when rHDL·YMOR was not coupled to G_{i2}, DAMGO competed [^{3}H]DPN binding with micromolar affinity (supplemental Fig. S2).

Just as YMOR membrane preparations displayed DAMGO-induced [^{35}S]GTPγS binding to G_{i2}, monomeric YMOR in rHDL particles showed strong DAMGO stimulation of nucleotide exchange (~4.7-fold stimulation with an EC_{50} of 31 $\pm$ 2.2 nM; Fig. 4*C*). A fluorescently labeled agonist, [Lys[7], Cys[8]]dermorphin-Cy3, was also tested and showed concentration-dependent stimulation of [^{35}S]GTPγS binding to G_{i2} by monomeric YMOR (EC_{50} of 32 $\pm$ 9.1 nM; supplemental Fig. S4*B*).

Although G_{i2} was added to rHDL·YMOR at a 10:1 molar ratio in these reconstitutions, the observed high and low agonist affinities illustrate that not all YMOR was coupled to G_{i2}. In fact, the agonist competition assays indicate that $\sim54\%$ of the receptor was coupled to G_{i2}. These data are consistent with previous studies on the β_2AR where the addition of purified G protein heterotrimer to rHDL particles in the absence of detergents resulted in 90–95% G protein loss, largely because of aggregation (14). Indeed, SEC analysis of rHDL·YMOR before and after G_{i2} addition confirmed that a large amount of the heterotrimer aggregates during its addition (data not shown). As such, the two populations of $\sim54\%$ coupled and $\sim46\%$

10 μM GTPγS (DAMGO (□), $K_{i\,GTP\gamma S} = \sim1$ μM; morphine (○), $K_{i\,GTP\gamma S} = \sim1$ μM). In both *A* and *B*, data were normalized to the maximal binding level as calculated by a one- or two-site competition curve fit (Prism 5.0, GraphPad). *C*, HDL-reconstituted YMOR in response to agonist binding. YMOR (an estimated 50–60 fmol) and associated G_{i2} heterotrimer were incubated with 10 nM [^{35}S]GTPγS (isotopically diluted) in the presence of increasing concentrations of DAMGO. DAMGO activated G_{i2} with an EC_{50} of 29 $\pm$ 1.4 nM, stimulating ~40 fmol of [^{35}S]GTPγS binding to $G\alpha_{i2}$ over basal levels, suggesting approximately a 1:0.7 coupling between YMOR and G protein. These results correlate with the estimated 53% high state observed in *B*. The data are representative of three experiments performed in duplicate. The *error bars* represent the standard error of the mean.
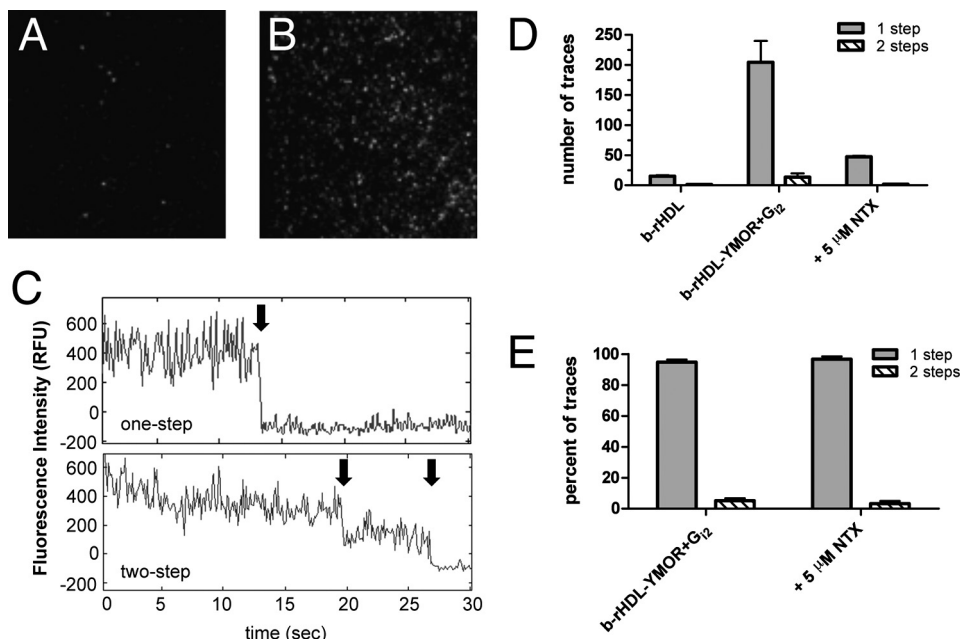
FIGURE 5. **Single-molecule imaging of Cy3-labeled agonist binding to rHDL·YMOR + G_{i2} confirms that the majority of YMOR is monomeric when reconstituted into HDL.** Binding of [Lys[7], Cys[8]]dermorphin-Cy3, a fluorescently labeled MOR-specific agonist, to rHDL·YMOR+G_{i2} was observed with prism-based total internal reflection fluorescence microscopy. YMOR was reconstituted into HDL particles using biotinylated apoA-1, followed by G_{i2} heterotrimer addition at a 30:1 G protein to receptor molar ratio. Reconstituted HDL (*A*) or rHDL·YMOR+G_{i2} (*B*) were then incubated with a saturating concentration (500 nM) of [Lys[7], Cys[8]]dermorphin-Cy3, adhered to a streptavidin-coated quartz slide, and washed with ice-cold 25 mM Tris·HCl, pH 7.7 buffer. Bound [Lys[7], Cys[8]]dermorphin-Cy3 was continuously excited at 532 nm to observe photobleaching of the fluorophore. *C*, representative fluorescence intensity traces for a one- and two-step photobleach event are shown. The *arrows* indicate photobleach events. *D* and *E*, quantification of photobleaching showed ~95% of the bound [Lys[7], Cys[8]]dermorphin-Cy3 bleached in a single step, suggesting that 95% of rHDL particles contained monomeric YMOR. [Lys[7], Cys[8]]dermorphin-Cy3 binding was reversible, as shown the addition of 5 μM NTX. A minimum of four slide regions and 200 fluorescent spots were counted for each sample.

DISCUSSION

Intense research over the past decade has focused on the existence and functional consequences of GPCR oligomerization. Recently, our laboratory and others have taken advantage of a unique phospholipid bilayer platform in the form of rHDL particles (13–16). Using this system we previously demonstrated the functional reconstitution of two prototypical GPCRs, rhodopsin and β₂AR (14, 15). Having illustrated that these receptors are monomeric following reconstitution, we observed complete functional coupling to their respective G proteins. For the β₂AR, agonist binding to monomeric receptor is allosterically regulated by the stimulatory heterotrimeric G protein $G\alpha_s\beta\gamma$. Therefore GPCR dimerization is not required for functional G protein coupling in the prototypical class A GPCRs rhodopsin and β₂AR.

In contrast, the accumulation of considerable biochemical and biophysical evidence suggests that the μ-, δ-, and κ-opioid receptors may function in a fashion that is dependent on their oligomerization. Analy-

uncoupled YMOR correspond well with the expected final G protein to YMOR ratio of 0.5–1:1.

Single-particle Visualization of Agonist Binding to rHDL·YMOR—[Lys[7], Cys[8]]dermorphin was used as an agonist probe to visualize binding to monomeric YMOR in rHDL at the single-molecule level with TIRF (Fig. 5). [Lys[7], Cys[8]]-dermorphin was labeled with a Cy3 fluorophore (supplemental Fig. S3), and its ability to bind reconstituted YMOR with high affinity and stimulate [³⁵S]GTPγS binding to $G\alpha_{i2}$ was confirmed (supplemental Fig. S4). YMOR was reconstituted with biotinylated Δ(1–43)-His₆-apoA-1 (b-rHDL·YMOR), enriched on a FLAG affinity column, and added to G_{i2} heterotrimer at a 30:1 G_{i2}:YMOR molar ratio to ensure complete receptor coupling to G protein. Binding of a saturating concentration (500 nM) of [Lys[7], Cys[8]]dermorphin-Cy3 to b-rHDL·YMOR+G_{i2} was then imaged with SM-TIRF. Fifty picomolar b-rHDL or b-rHDL·YMOR+G_{i2} (Fig. 5, *A* and *B*) samples were continuously excited at 532 nm and fluorescence intensity traces (Fig. 5C) were analyzed for step photobleaching. Approximately 95% of the b-rHDL·YMOR+G_{i2} fluorescence traces exhibited single-step photobleaching, suggesting that a single [Lys[7], Cys[8]]dermorphin-Cy3 was localized within each fluorescent spot (Fig. 5, *D* and *E*). Having shown that rHDL particles contain a single receptor, these photobleaching data indicate that only one dermorphin bound per receptor.

sis of receptor overexpression in co-transfected cells suggested the existence of δ-δ homodimers (34) and demonstrated unique pharmacology resulting from μ-δ (6, 7, 10) and δ-κ heterodimers (35). Bioluminescence resonance energy transfer studies have shown that homo- and heterodimers can be formed by all three opioid receptor isoforms (8). These findings have promoted the notion that opioid receptor oligomerization is important for function (36, 37). However, with co-transfection systems the final profiles of μ and δ monomers, homodimers, and heterodimers are unknown. In light of these reports, we rationalized that it was vital to determine whether the monomeric form of the MOR behaves in a pharmacologically similar manner as the native, membrane-bound form.

The HDL reconstitution system was used to investigate the function of monomeric MOR. Reconstitution of MOR required the purification of active receptor in large enough quantities for subsequent biochemical manipulation and analysis. Previous reports of MOR purification from endogenous or recombinant sources have yielded either low quantities (38–42) or poor agonist binding affinities (43–45). Several aspects were key to the expression and purification of YFP-MOR (YMOR): a cleavable hemagglutinin signal sequence at the N terminus of the receptor (46), the presence of naltrexone during expression, and the inclusion of cholesteryl hemisuccinate and naltrexone during the entire purification process. These modifications contrib-

Functional G Protein Coupling by μ-Opioid Receptor Monomer

uted to the stabilization of YMOR, leading to an increase in yields during the chromatography process as well as increasing the specific activity of the detergent solubilized receptor. Reconstitution into HDL facilitated the isolation of a monomeric form of YMOR that couples to and activates heterotrimeric G proteins. Furthermore, we illustrate that the inhibitory G protein $G\alpha_i\beta\gamma$ can allosterically regulate agonist binding to monomeric MOR. These results suggest that G protein regulation of monomeric receptors is likely a phenomenon common to all G proteins and class A GPCRs. The capacity of MOR to couple to various isoforms of $G_{i/o}$ heterotrimers in a differential manner are currently under investigation in our laboratory.

Taken together our results demonstrate the functionality of monomeric MOR, illustrating that the opioid GPCR does not require dimerization to bind ligands and signal to G proteins. However, these data do not refute the existence of opioid receptor oligomerization in cells. It remains possible that homo- and heterodimerization create unique ligand binding entities that may be subject to differential regulation, desensitization, and internalization. One of our future goals is to isolate various oligomeric states of opioid receptors and other GPCRs in rHDL particles and compare their activities toward ligands and signaling partners directly. A major technical obstacle is the formation of "anti-parallel" receptor dimers, where the N termini for the reconstituted GPCRs in the oligomer are on opposite sides of the phospholipid bilayer. Indeed, reconstitution of two GPCRs in a single rHDL particle has been previously demonstrated for rhodopsin (13, 16), but a detailed analysis by nanogold labeling and single-particle electron microscopy of the reconstituted "dimers" reveals that a significant fraction were anti-parallel (16). It is plausible, and even likely, that an anti-parallel GPCR dimer will result in suboptimal or disrupted G protein coupling. The development of approaches to ensure parallel GPCR dimer incorporation into rHDL particles to confidently study the functional relevance of opioid receptor dimerization is currently a major priority in the laboratory.

HDL reconstitution of YMOR also provided a platform for analysis of ligand binding using single-molecule microscopy. In this study we examined the reversible binding of a μ-opioid receptor specific agonist [Lys[7], Cys[8]]dermorphin (47) with SM-TIRF. To the best of our knowledge these data represent the first reported observation of a peptide agonist binding to an isolated GPCR in a lipid bilayer using single-particle imaging. We are currently refining our methods to resolve the kinetics of ligand binding to YMOR, as well as visualizing ligand binding to opioid receptors in intact cells. Peptide receptors such as the opioid family are particularly amenable to fluorescence spectroscopy because the relatively large ligand size can tolerate the incorporation of fluorophores without drastically impairing binding affinities. This single-molecule visual approach of studying ligand binding to opioid receptors, utilizing labeled agonists and antagonists with unique binding affinities toward receptor homo- and heterodimers, may potentially address opioid receptor oligomerization in physiologically relevant tissue preparations.

REFERENCES

1. Blume, A. J., Lichtshtein, D., and Boone, G. (1979) *Proc. Natl. Acad. Sci. U.S.A.* **76,** 5626–5630
2. North, R. A., Williams, J. T., Surprenant, A., and Christie, M. J. (1987) *Proc. Natl. Acad. Sci. U.S.A.* **84,** 5487–5491
3. Waldhoer, M., Bartlett, S. E., and Whistler, J. L. (2004) *Annu. Rev. Biochem.* **73,** 953–990
4. Bai, M. (2004) *Cell Signal.* **16,** 175–186
5. Milligan, G., Canals, M., Pediani, J. D., Ellis, J., and Lopez-Gimenez, J. F. (2006) *Ernst Schering Found. Symp. Proc.* **2,** 145–161
6. George, S. R., Fan, T., Xie, Z., Tse, R., Tam, V., Varghese, G., and O'Dowd, B. F. (2000) *J. Biol. Chem.* **275,** 26128–26135
7. Martin, N. A., and Prather, P. L. (2001) *Mol. Pharmacol* **59,** 774–783
8. Wang, D., Sun, X., Bohn, L. M., and Sadée, W. (2005) *Mol. Pharmacol.* **67,** 2173–2184
9. Gomes, I., Filipovska, J., Jordan, B. A., and Devi, L. A. (2002) *Methods* **27,** 358–365
10. Gomes, I., Jordan, B. A., Gupta, A., Trapaidze, N., Nagy, V., and Devi, L. A. (2000) *J. Neurosci.* **20,** RC110
11. Leitz, A. J., Bayburt, T. H., Barnakov, A. N., Springer, B. A., and Sligar, S. G. (2006) *BioTechniques* **40,** 601–606
12. Nath, A., Atkins, W. M., and Sligar, S. G. (2007) *Biochemistry* **46,** 2059–2069
13. Bayburt, T. H., Leitz, A. J., Xie, G., Oprian, D. D., and Sligar, S. G. (2007) *J. Biol. Chem.* **282,** 14875–14881
14. Whorton, M. R., Bokoch, M. P., Rasmussen, S. G., Huang, B., Zare, R. N., Kobilka, B., and Sunahara, R. K. (2007) *Proc. Natl. Acad. Sci. U.S.A.* **104,** 7682–7687
15. Whorton, M. R., Jastrzebska, B., Park, P. S., Fotiadis, D., Engel, A., Palczewski, K., and Sunahara, R. K. (2008) *J. Biol. Chem.* **283,** 4387–4394
16. Banerjee, S., Huber, T., and Sakmar, T. P. (2008) *J. Mol. Biol.* **377,** 1067–1081
17. Liang, Y., Fotiadis, D., Filipek, S., Saperstein, D. A., Palczewski, K., and Engel, A. (2003) *J. Biol. Chem.* **278,** 21655–21662
18. Fotiadis, D., Liang, Y., Filipek, S., Saperstein, D. A., Engel, A., and Palczewski, K. (2003) *Nature* **421,** 127–128
19. Jastrzebska, B., Fotiadis, D., Jang, G. F., Stenkamp, R. E., Engel, A., and Palczewski, K. (2006) *J. Biol. Chem.* **281,** 11917–11922
20. Schaffner, W., and Weissmann, C. (1973) *Anal. Biochem.* **56,** 502–514
21. Kozasa, T. (1999) in *G Proteins: Techniques of Analysis* (Manning, D. R., ed) pp. 23–28, CRC Press, Boca Raton, FL
22. Patil, P. V., and Ballou, D. P. (2000) *Anal. Biochem.* **286,** 187–192
23. Emmerson, P. J., Clark, M. J., Mansour, A., Akil, H., Woods, J. H., and Medzihradsky, F. (1996) *J. Pharmacol. Exp. Ther* **278,** 1121–1127
24. Alt, A., Mansour, A., Akil, H., Medzihradsky, F., Traynor, J. R., and Woods, J. H. (1998) *J. Pharmacol. Exp. Ther.* **286,** 282–288
25. Clark, M. J., Furman, C. A., Gilson, T. D., and Traynor, J. R. (2006) *J. Pharmacol. Exp. Ther.* **317,** 858–864
26. Frances, B., Moisand, C., and Meunier, J. C. (1985) *Eur. J. Pharmacol.* **117,** 223–232
27. Werling, L. L., Puttfarcken, P. S., and Cox, B. M. (1988) *Mol. Pharmacol.* **33,** 423–431
28. Ott, S., and Costa, T. (1989) *Biochem. Pharmacol.* **38,** 1931–1939
29. Richardson, A., Demoliou-Mason, C., and Barnard, E. A. (1992) *Proc. Natl. Acad. Sci. U.S.A.* **89,** 10198–10202
30. Kenakin, T. (2004) *Trends Pharmacol. Sci.* **25,** 186–192
31. Rosenbaum, D. M., Cherezov, V., Hanson, M. A., Rasmussen, S. G., Thian, F. S., Kobilka, T. S., Choi, H. J., Yao, X. J., Weis, W. I., Stevens, R. C., and Kobilka, B. K. (2007) *Science* **318,** 1266–1273
32. Cho, T. M., Ge, B. L., and Loh, H. H. (1985) *Life Sci.* **36,** 1075–1085
33. Ramon, E., Marron, J., del Valle, L., Bosch, L., Andrés, A., Manyosa, J., and Garriga, P. (2003) *Vision Res.* **43,** 3055–3061
34. Cvejic, S., and Devi, L. A. (1997) *J. Biol. Chem.* **272,** 26959–26964
35. Jordan, B. A., and Devi, L. A. (1999) *Nature* **399,** 697–700
36. Levac, B. A., O'Dowd, B. F., and George, S. R. (2002) *Curr. Opin Pharmacol.* **2,** 76–81
37. Milligan, G. (2004) *Mol. Pharmacol.* **66,** 1–7

38. Gioannini, T. L., Howard, A. D., Hiller, J. M., and Simon, E. J. (1985) *J. Biol. Chem.* **260,** 15117–15121

39. Li, L. Y., Zhang, Z. M., Su, Y. F., Watkins, W. D., and Chang, K. J. (1992) *Life Sci.* **51,** 1177–1185

40. Talmont, F., Sidobre, S., Demange, P., Milon, A., and Emorine, L. J. (1996) *FEBS Lett.* **394,** 268–272

41. Obermeier, H., Wehmeyer, A., and Schulz, R. (1996) *Eur. J. Pharmacol.* **318,** 161–166

42. Massotte, D., Baroche, L., Simonin, F., Yu, L., Kieffer, B., and Pattus, F. (1997) *J. Biol. Chem.* **272,** 19987–19992

43. Sarramegna, V., Demange, P., Milon, A., and Talmont, F. (2002) *Protein Expr. Purif.* **24,** 212–220

44. Sarramegna, V., Talmont, F., Seree de Roch, M., Milon, A., and Demange, P. (2002) *J. Biotechnol.* **99,** 23–39

45. Sarramegna, V., Muller, I., Mousseau, G., Froment, C., Monsarrat, B., Milon, A., and Talmont, F. (2005) *Protein Expr. Purif.* **43,** 85–93

46. Guan, X. M., Kobilka, T. S., and Kobilka, B. K. (1992) *J. Biol. Chem.* **267,** 21995–21998

47. Attila, M., Salvadori, S., Balboni, G., Bryant, S. D., and Lazarus, L. H. (1993) *Int. J. Pept. Protein Res.* **42,** 550–559